Resonances and Dissociative Electron Attachment in HNCO

M. Zawadzki,[1,2] M. Čížek,[3,*] K. Houfek,[3] R. Čurík,[1] M. Ferus,[1] S. Civiš,[1] J. Kočišek,[1] and J. Fedor[1,†]

[1]*J. Heyrovský Institute of Physical Chemistry, Czech Academy of Sciences, Dolejškova 3, 18223 Prague, Czech Republic*
[2]*Department of Atomic, Molecular and Optical Physics, Faculty of Applied Physics and Mathematics,*
Gdańsk University of Technology, ul. G. Narutowicza 11/12, 80-233 Gdańsk, Poland
[3]*Faculty of Mathematics and Physics, Charles University, Institute of Theoretical Physics,*
V Holešovičkách 2, 18000 Prague, Czech Republic

In a combined experimental and theoretical study, we probe the dissociative electron attachment in isocyanic acid HNCO. The experimental absolute cross section for the NCO^- fragment shows a sharp onset and fine structures near the threshold. The autoionizing state responsible for the dissociative attachment is found in both the R-matrix calculation and using analytic continuation in the coupling constant. The involved A' resonance has a mixed π^*/σ^* character along the dissociating bond and thus combines the effects of nonzero electron angular momentum and dipole-supported states. This leads to unusual behavior of its width at various geometries. Because the potential energy gradient of the autoionizing state points essentially in the direction of the N─H bond, nuclear dynamics can be described by a one-dimensional nonlocal model. The results agree with the experiment both quantitatively and qualitatively. The present system may be a prototype for interpretation of the dissociative electron attachment process in a number of other polyatomic systems.

Dissociative electron attachment (DEA) represents the only way of breaking a molecular bond at impact energies below the electronic excitation threshold. It thus drives the chemical transformation in a number of environments with a high abundance of slow electrons, both where these are primary species (low-temperature plasmas, focused-beam nanofabrication) or where these are secondary species resulting from the interaction of high-energy radiation with matter (radiation damage in biological tissue, astrochemical synthesis). At the same time, our understanding of DEA for polyatomic molecules is surprisingly small. DEA proceeds via the formation of resonances—transient anions—embedded in a continuum. Such temporary anion states give rise to a strong coupling of electronic and nuclear motion and nonadiabatic phenomena [1].

Saturated polyatomic molecules with low dipole moments have usually negligible DEA cross sections at low electron energies (below the onset of the core-excited resonances). The reason is that such systems allow only for formation of σ^* resonances with a weak barrier toward the electron autodetachment. Based on the simplified picture of dissociation and detachment competition, very few stable anion fragments are produced. Many unsaturated or strongly polar molecules, on the other hand, show very high cross sections for production of the dehydrogenated closed-shell anions $(M-H)^-$. In this case, the dissociative cross section is dramatically increased for two reasons. First, target molecules with double or triple bonds possess low-lying unoccupied orbitals of π^* character. They give rise to much narrower π^* resonances with the detachment channel strongly suppressed. Second, in the case of molecules with sufficiently strong dipole moment or high polarizability, their long-range interaction dramatically enhances the dissociative cross section even for the σ^* states, due to the interaction of these broad resonances with long-range-supported bound or virtual states [2]. The relative importance of these two mechanisms of electron-impact molecular dissociation has been a matter of an intensive debate [1,3–5].

Part of the controversy lies in the incomplete theory: due to necessary approximations, the two mechanisms have been so far described by distinctly different approaches. The first approach is based on a local complex potential approximation, in which the resonance width is a function of the nuclear coordinates only. Such a simplification results in two major consequences. The positive one is that it computationally allows for the multidimensional treatment of nuclear dynamics. This is actually a necessity in many model target systems with π^* resonances where the dissociation requires symmetry lowering, such as out-of-line (as in acetylene [6] or hydrogen cyanide [7]) or out-of-plane motion (as in formic acid [3]), in addition to the bond stretching. The negative consequence is the failure to describe the effects due to the long-range interactions. These interactions are well underpinned in the second class of theoretical approaches: the nonlocal resonance theory [8] and the effective range R-matrix theory [9,10]. In these, the resonance width is additionally a function of the electron

energy. Both methods have been successful in reproducing phenomena resulting from the nonlocal and nonadiabatic effects [11,12]. However, in the case of DEA, they have been developed only for one-dimensional problems. The extended R-matrix theory has been applied to polyatomics, which were treated as pseudodiatomics [4,13,14], and only the resonant states with a σ^* symmetry along the stretching polar bond were taken into account.

In this Letter we address a question whether π^* resonances, that become dissociative during the geometry distortion, can give rise to similar structures that were observed for the pure σ^* states.

The equilibrium geometry of isocyanic acid, HNCO, (HNC angle of 124°) *a priori* mixes the two described mechanisms and symmetries and thus represents a good target system to answer this question. Apart from being a fundamentally interesting target, the electron-induced decomposition of this molecule is of high astrophysical interest. It is the simplest molecule containing the four basic life-forming chemical elements, and it has been detected in a number of interstellar environments: interstellar clouds [15–17], young stellar objects [18], molecular outflows [19], and comets [20]. As such, it has been attracting attention as a possible prebiotic precursor [21,22] in formation of the peptide bond. It is believed that in the interstellar space the reactions are to a large degree initiated by ultraviolet light, x-rays, and cosmic rays. When all these interact with interstellar icy grains that serve as reservoirs for chemical species, an avalanche of secondary electrons is produced, thereby setting the stage for the DEA as a molecular decomposition trigger.

Experimentally, the HNCO sample was synthesized by a pyrolysis of cyanouric acid [23,24]. During the measurements, the sample was kept at the temperature of solid CO_2 ($-78.5\,°C$), only slightly above the HNCO melting temperature ($-86\,°C$). We used two complementary setups: DEA spectrometer with a quadrupole mass filter [25,26] which measures high-resolution ion yield (incident beam resolution of 100 meV) and quantitative DEA spectrometer with a time-of-flight analyzer which measures absolute cross sections [27,28]. The energy scale and the absolute cross sections were normalized against the 4.4 eV resonance in the O^- production from CO_2 [5]. The spectra obtained from the first setup were normalized to the time-of-flight absolute values in a way as to conserve the areas under the bands. The uncertainty of the absolute value (2σ) is estimated to be $\pm25\%$.

Red line in Fig. 1 shows the absolute cross section for the only DEA channel detected, hydrogen abstraction $HNCO + e^- \rightarrow NCO^- + H$. The threshold E_{th} is 1.16 eV, as determined by the H—NCO bond dissociation energy of 4.77 eV [29] and NCO electron affinity of 3.61 eV [30]. The NCO^- signal appears at this threshold with a vertical onset. The spectrum shows pronounced features close to this onset and drops fast above 3 eV.
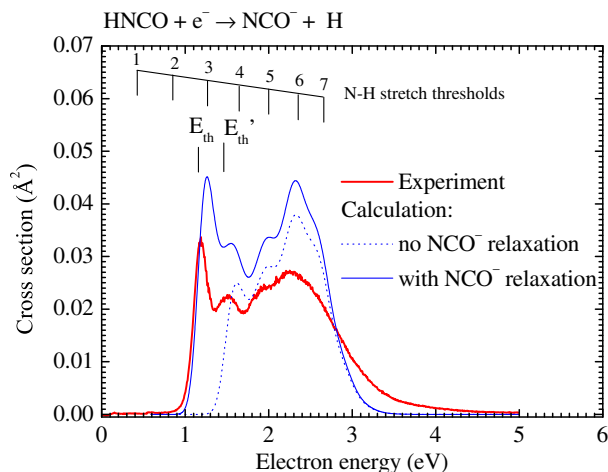

FIG. 1. Red: experimental DEA cross section for the NCO^- production from HNCO. Blue: calculated cross sections, with two different threshold energies, convoluted with a Gaussian of 200 meV FWHM. The results for E'_{th} do not take into account the asymptotic NCO^- relaxation into linear geometry, whereas the data for E_{th} account for this relaxation.

To characterize the involved potential energy surfaces, we have adopted several approaches. The electronically bound states were computed with the coupled-clusters approach CCSD-T/aug-cc-pVTZ [31–33]. The states embedded in a continuum were characterized in the following two ways: (i) by the regularized analytic continuation (RAC) method [34,35] and (ii) R-matrix scattering calculations. The method (i) applies an attractive perturbation potential which, if sufficiently strong, turns the resonance into a bound state which can be described by the standard CCSD-T method [36]. The complex resonant energy is obtained by a continuation to the limit of zero perturbation potential. Resulting resonance parameters for the equilibrium geometry are $E_r = 2.49$ eV and $\Gamma = 0.48$ eV. In the method (ii) we performed fixed-nuclei R-matrix calculations [37] as implemented in the UK molecular R-matrix suite of codes [38,39]. We employed the static-exchange plus polarization model [37] in which the target molecule is described on the Hartree-Fock level in the cc-pVDZ basis. This model is justified for energies of interest because the first electronic excited state of HNCO lies more than 5 eV above the ground electronic state at the equilibrium geometry. The number of virtual orbitals, which controls a level of electronic correlation included in the scattering calculation, was set to 17 by comparison of the R-matrix potential energy curves with the CCSD-T results.

Figure 2 shows the potential energy surfaces obtained by these methods. The top panel displays the one-dimensional cut along the N—H bond, and the bottom panel compares it with bending the HNC angle. The bound anion curve at long N—H distances in Fig. 2(a) ends slightly above the asymptotic dissociation threshold due to missing relaxation
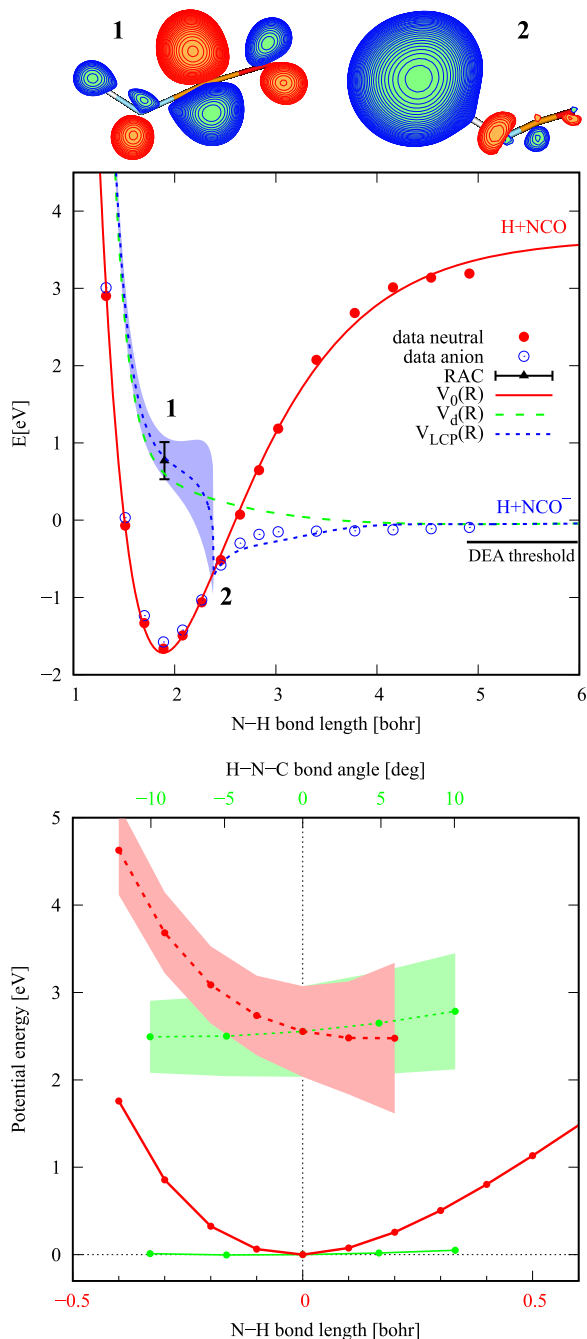
FIG. 2. Involved potential energy surfaces. (a) Cut along the N—H bond with the HNC angle kept fixed. The orbitals shown at two different geometries labeled 1 and 2 are singly occupied HNCO⁻ orbitals in the reference determinant used in the CCSD-T calculations. Blue shaded region indicates the width of the resonance from the local complex potential approximation to the final nonlocal model. RAC calculation including width is also shown as black error bar. (b) Comparison of the cuts along the N—H bond (red) and along the bending of the HNC angle (green). Here the widths are obtained by fitting the Breit-Wigner formula using the R-matrix codes.

of the remaining NCO⁻ anion (NCO⁻ relaxes to the linear geometry during the dissociative process). With the shortening of the bond, the anion curve bends down up to the

crossing point. This is a typical behavior in systems which generate a sufficiently strong dipole moment to support dipole-bound states only at extended bond length. The dominant electronic configuration of HNCO⁻ is that of a diffuse weakly bound state. In the neutral equilibrium geometry, the electronic configuration is of A' symmetry; however, from the point of view of the N—H bond the resonance has a mixed σ^*/π^* character.

Dependence of the resonant potential surface on the HNC bending angle is much flatter—the scales on top and bottom axes in Fig. 2(b) are chosen in such a way that we can directly compare the gradient of the resonant energy E_r in the two directions. Figure 2(b) demonstrates that the dynamics is essentially one dimensional and that it will proceed mainly along the N—H bond. The curve-crossing behavior resembles situation in hydrogen halides, where the nonlocal model was successful in the qualitative and quantitative DEA description [11,12]. The central assumption of the nonlocal resonance model is that all the nonadiabatic coupling responsible for the DEA can be described in a diabatic representation represented by one discrete state $|\phi_d\rangle$ crossing into the continuum of electron scattering states $|\phi_\epsilon\rangle$. Both the discrete state and continuum states depend parametrically on the molecular geometry, here constituted by the N—H bond length R. In the present system, the discrete state $|\phi_d\rangle$ is characterized by the electronic bound state (H + NCO⁻) for large values R and by the resonance for R close to equilibrium N—H bond length.

The nonlocal resonance model is fully described by knowledge of the potentials $V_0(R)$, $V_d(R)$, and the coupling element $V_{d\epsilon}(R)$. The potential of the neutral molecule $V_0(R)$, shown by the red line in Fig. 2(a), was fitted to the energies obtained by the CCSD-T method (red points). The potential $V_d(R)$ should closely follow the negative ion bound state energy or resonance position, whenever the coupling $V_{d\epsilon}$ is small. The determination of the coupling element $V_{d\epsilon}(R)$ and fine tuning of the discrete-state potential close to the crossing of $V_0(R)$ and $V_d(R)$ are performed by fitting R-matrix eigenphase sums to the generalized Breit-Wigner formula

$$\delta(R,\epsilon) = \delta_{\mathrm{BG}}(R,\epsilon) + \arctan\frac{\Gamma(R,\epsilon)/2}{\epsilon - V_d(R) - \Delta(R,\epsilon)}, \quad (1)$$

where δ_{BG} is the background phase shift with known threshold behavior. The coupling $V_{d\epsilon}(R)$ of continuum to the discrete state is related to the width as $\Gamma = 2\pi|V_{d\epsilon}(R)|^2$. Furthermore, the level shift Δ is uniquely determined from Γ by means of the Hilbert transform. The resulting fit shown in Fig. 3 reproduces the R-matrix data very well. The details of the functional form and resulting fitting parameters are given in Supplemental Material [40].

Figure 2(a) provides visualization of the resulting nonlocal resonance model by showing potentials associated with the model as described in the figure caption. The potential V_{LCP} and the width are given by real and
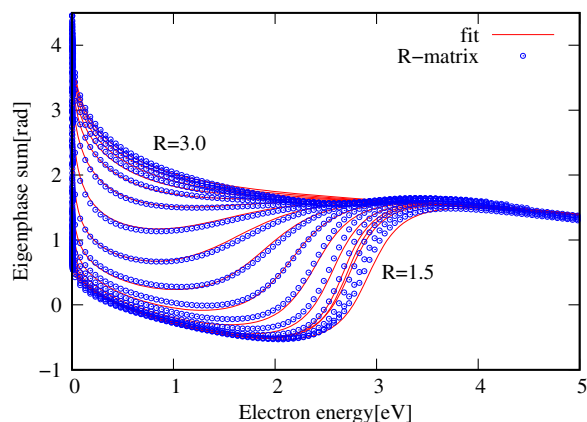
FIG. 3. Calculated R-matrix eigenphase sums (dots) for the N—H bond length $R = 1.5, 1.6, \ldots, 3.0$ bohr and the corresponding fits from the generalized Breit-Wigner formula (lines).

imaginary part of the local potential approximation to the nonlocal model [8]. Note the unusual shape of width, which becomes very broad close to the threshold. This is a consequence of the over-critical dipole moment of the molecule, because the coupling element $V_{d\epsilon}$ does not vanish at threshold $\epsilon = 0$. Furthermore, the resonance narrows when it gains a valence character for shorter N—H bond distances. This behavior is reflected by two terms in the fit of coupling function $V_{dE}(R) = g_1(1 + g_2\sqrt{E})e^{-\beta E}$ (see the Supplemental Material [40]), which may mimic contribution of two partial waves.

The cross sections within the nonlocal resonance model are calculated using standard procedures as described e.g., in the review [8]. The computational details and fitting process closely follow that for DEA in hydrogen halides [11,12].

Figure 1 compares the calculated DEA cross section with the experimental data. In the model strictly constructed as described above, the missing relaxation of the NCO$^-$ causes a higher DEA threshold E_{th}', effectively cutting off the low-energy peak in the calculated spectrum. In order to account for this relaxation, we have shifted the anion curve by 300 meV to lower energies to reproduce correctly the relaxed DEA threshold. As demonstrated in Supplemental Material [40], such a shift only changes the threshold peak but does not influence much the cross section at higher energies. Qualitatively, the model reproduces all the fine features in the experimental spectrum. Quantitatively, the calculated cross section is approximately by 30% higher than the experimental one. In view of the extreme sensitivity of the cross-section values on the resonance width [12], this level of quantitative agreement can be considered excellent, especially for the model based on the first principles.

The origin of the fine structures in the cross section is related to the fact, that the vibrational excitation cross sections for polar molecules show strong threshold peaks [41]. Because of interchannel coupling, the sharp onset of the vibrational excitation cross sections is manifested as

structure in the DEA cross section at energies corresponding to opening of these channels. Positions of the structures correspond to vibrational thresholds of the N-H stretching mode. Their accurate reconstruction by the theory further supports plausibility of the single nuclear reaction coordinate.

The present findings shed a new light on the problem of DEA hydrogen abstraction in several polyatomic molecules that have been discussed in recent years.

(i) Hydrogen cyanide HCN is a linear molecule. It has been theoretically described within the local complex approximation: in the model of Chourou and Orel [7], the formation of the π^* resonance leads to distortion of the linear geometry and leaving hydrogen bends out of line. The magnitude of the calculated cross section reasonably agreed with the experimental data [42]; however, the isotope effect and especially the weak fine experimental structures were not reproduced by the model. Upon the initial bend, the electronic situation becomes equivalent to HNCO with the mixed symmetries. The observed structures may, thus, originate from the nonlocal effects, similar as in the present case, and not from the CN$^-$ fragment excitation as ascribed previously [42].

(ii) Formic acid HCOOH, which loses hydrogen from the oxygen site producing HCOO$^-$, has attracted an intensive debate. The calculations of potential energy surfaces in the local complex approximation suggested [3] that the DEA proceeds via formation of the π^* resonance and subsequent geometry distortion, mediated by the H atom which is not dissociating. However, it has been shown experimentally [5] that the motion of this atom has only a small (but observable) effect on the final cross-section magnitude. The model assuming a dipole-supported σ^* resonance and no geometry distortion has very well reproduced both the magnitude and the fine features in the spectra [4]. However, it somewhat overestimates the isotope effect [2] of the O—D deuterated compound. The multidimensionality of the problem might be the answer: upon any geometry distortion, the π^*/σ^* states become mixed along the polar dissociating OH bond, thus resembling the present case. The observed fine structures would be thus not present only in the one-dimensional in-plane motion, but can be caused by the nonlocal effects in the dissociating resonance of the mixed symmetry such as in HNCO.

(iii) Uracil dehydrogenation yield is remarkably similar to the present cross section [43,44]. A lot of effort has been put into the identification of the individual features. Gallup and Fabrikant [13] applied a one-dimensional model based on the dipole-supported σ^* resonance. The model reproduced the fine features in the DEA spectrum; however, as the authors concluded, the part of the spectrum due to the π^* resonance associated with the double bond system was completely missing in their calculations. Also, in this case we believe that the two processes cannot be considered separately, upon breaking the planar symmetry they

become indistinguishable and, as in the present case, the whole spectrum should be interpreted in a unified way.

A note should be added to the two latter cases: there, the π^* refers to the A'' symmetry, antisymmetric with respect to the equilibrium molecular plane. In HNCO, π^* refers to the A' state. The analogy between the two cases appears when the out-of-plane motion in formic acid or uracil mixes the plane-symmetric and antisymmetric states.

In conclusion, we have shown that the experimental DEA cross section in HNCO is very well reproduced within the nonlocal resonance theory. The anion state described in this way stems from the interaction of A' resonance (mixed σ^*/π^* along the N—H bond) and the dipole-bound state at the prolonged N—H distance. The high level of agreement suggests that the failure of reproducing the fine structures in the models assuming formation of π^* resonances in polyatomic molecules is not due to the wrong assumption of the involved electronic states, but merely due to local complex approximation used in these models.

---

[*]cizek@mbox.troja.mff.cuni.cz

[†]juraj.fedor@jh-inst.cas.cz

[1] I. I. Fabrikant, S. Eden, N. J. Mason, and J. Fedor, Adv. At. Mol. Opt. Phys. **66**, 545 (2017).

[2] I. I. Fabrikant, J. Phys. B **49**, 222005 (2016).

[3] T. N. Rescigno, C. S. Trevisan, and A. E. Orel, Phys. Rev. Lett. **96**, 213201 (2006).

[4] G. A. Gallup, P. D. Burrow, and I. I. Fabrikant, Phys. Rev. A **79**, 042701 (2009).

[5] R. Janečková, D. Kubala, O. May, J. Fedor, and M. Allan, Phys. Rev. Lett. **111**, 213201 (2013).

[6] S. T. Chourou and A. E. Orel, Phys. Rev. A **77**, 042709 (2008).

[7] S. T. Chourou and A. E. Orel, Phys. Rev. A **83**, 032709 (2011).

[8] W. Domcke, Phys. Rep. **208**, 97 (1991).

[9] I. I. Fabrikant, S. A. Kalin, and A. K. Kazansky, J. Chem. Phys. **95**, 4966 (1991).

[10] I. I. Fabrikant and H. Hotop, Phys. Rev. Lett. **94**, 063201 (2005).

[11] M. Čížek, J. Horáček, A.-C. Sergenton, D. B. Popović, M. Allan, W. Domcke, T. Leininger, and F. X. Gadea, Phys. Rev. A **63**, 062710 (2001).

[12] J. Fedor, C. Winstead, V. McKoy, M. Čížek, K. Houfek, P. Kolorenč, and J. Horáček, Phys. Rev. A **81**, 042702 (2010).

[13] G. A. Gallup and I. I. Fabrikant, Phys. Rev. A **83**, 012706 (2011).

[14] V. Vizcaino, B. Puschnigg, S. E. Huber, M. Probst, I. I. Fabrikant, G. A. Gallup, E. Illenberger, P. Scheier, and S. Denifl, New J. Phys. **14**, 043017 (2012).

[15] L. E. Snyder and D. Buhl, Astrophys. J. **177**, 619 (1972).

[16] R. L. Brown, Astrophys. J. **248**, L119 (1981).

[17] B. E. Turner, R. Terzieva, and E. Herbst, Astrophys. J. **518**, 699 (1999).

[18] S. E. Bisschop, J. K. Jorgensen, E. F. van Dishoeck, and E. B. M. de Wachter, Astron. Astrophys. **465**, 913 (2007).

[19] N. J. Rodriguez-Fernandez, M. Tafalla, F. Gueth, and R. Bachiller, Astron. Astrophys. **516**, A98 (2010).

[20] D. C. Lis, J. Keene, K. Young, T. G. Phillips, D. Bockelée-Morvan, J. Crovisier, P. Schilke, P. F. Goldsmith, and E. A. Bergin, Icarus **130**, 355 (1997).

[21] G. Fedoseev, S. Ioppolo, D. Zhao, T. Lamberts, and H. Linnartz, Mon. Not. R. Astron. Soc. **446**, 439 (2015).

[22] L. Song and J. Kastner, Phys. Chem. Chem. Phys. **18**, 29278 (2016).

[23] G. Fischer, J. Geith, T. M. Klapotke, and B. Krumm, Z. Naturforsch **57**, 19 (2002).

[24] M. Ferus, V. Laitl, A. Knížek, P. Kubelík, J. Šponer, J. Kára, J. E. Šponer, B. Lefloch, G. Cassone, and S. Civiš, Astron. Astrophys. (to be published).

[25] M. Stepanović, Y. Pariat, and M. Allan, J. Chem. Phys. **110**, 11376 (1999).

[26] M. Zawadzki, M. Ranković, J. Kočišek, and J. Fedor, Phys. Chem. Chem. Phys. **20**, 6838 (2018).

[27] J. Fedor, O. May, and M. Allan, Phys. Rev. A **78**, 032701 (2008).

[28] O. May, J. Fedor, B. C. Ibănescu, and M. Allan, Phys. Rev. A **77**, 040701(R) (2008).

[29] B. Ruscic and J. Berkowitz, J. Chem. Phys. **100**, 4498 (1994).

[30] S. E. Bradforth, E. H. Kim, D. W. Arnold, and D. M. Neumark, J. Chem. Phys. **98**, 800 (1993).

[31] P. J. Knowles, C. Hampel, and H.-J. Werner, J. Chem. Phys. **99**, 5219 (1993).

[32] M. J. O. Deegan and P. J. Knowles, Chem. Phys. Lett. **227**, 321 (1994).

[33] T. H. Dunning, J. Chem. Phys. **90**, 1007 (1989).

[34] J. Horáček, I. Paidarová, and R. Čurík, J. Phys. Chem. A **118**, 6536 (2014).

[35] J. Horáček, I. Paidarová, and R. Čurík, J. Chem. Phys. **143**, 184102 (2015).

[36] R. Čurík, I. Paidarová, and J. Horáček, Eur. Phys. J. D **70**, 146 (2016).

[37] J. Tennyson, Phys. Rep. **491**, 29 (2010).

[38] L. A. Morgan, J. Tennyson, and C. J. Gillan, Comput. Phys. Commun. **114**, 120 (1998).

[39] J. M. Carr, P. G. Galiatsatos, J. D. Gorfinkiel, A. G. Harvey, M. A. Lysaght, D. Madden, Z. Mašín, M. Plummer, J. Tennyson, and H. N. Varambhia, Eur. Phys. J. D **66**, 58 (2012).

[40] See Supplemental Material at http://link.aps.org/supplemental/10.1103/PhysRevLett.121.143402 for the parameters of nonlocal resonance model and for the

sensitivity analysis of cross section on the asymptotic energy shift.

[41] K. Rohr and F. Linder, J. Phys. B **8,** L200 (1975).

[42] O. May, D. Kubala, and M. Allan, Phys. Rev. A **82,** 010701(R) (2010).

[43] G. Hanel, B. Gstir, S. Denifl, P. Scheier, M. Probst, B. Farizon, M. Farizon, E. Illenberger, and T. D. Märk, Phys. Rev. Lett. **90,** 188104 (2003).

[44] P. D. Burrow, G. A. Gallup, A. M. Scheer, S. Denifl, S. Ptasińska, T. D. Märk, and P. Scheier, J. Chem. Phys. **124,** 124310 (2006).